This article is published as part of a themed issue of ***Photochemical & Photobiological Sciences*** of contributions from:

6th European Meeting on Solar Chemistry and Photocatalysis: Environmental Applications

Guest edited by **Josef Krysa** and **Sixto Malato**

Published in **issue 3, 2011**

Papers

Degradation of dichloroacetic acid in homogeneous aqueous media employing ozone and UVC radiation†

María Eugenia Lovato,* Carlos A. Martín and Alberto E. Cassano

Received 5th July 2010, Accepted 12th August 2010
DOI: 10.1039/c0pp00208a

A tentative workable mechanism for dichloroacetic acid decomposition (DCA) in aqueous media employing ozone and UVC radiation has been developed. All experiments were made in a homogeneous medium under assured kinetic control regime. Under no circumstances did a headspace exist in the reactor volume. The starting point of the reaction with UVC radiation was always under the prerequisite of a confirmed state of initial equilibrium conditions for the mixture water-ozone-oxygen at 20 °C. The explored variables were: (i) DCA initial concentration, (ii) ozone concentration and (iii) fluence rate at the reactor window. The model comprises three parallel reactions: (1) direct photolysis, (2) direct ozonation and (3) ozone + UVC degradation. Complete DCA removal was achieved, and the mass balance, considering DCA disappearance and chloride ion formation, closed within very small error. The combination of ozone and UVC radiation produces a significant amount of hydrogen peroxide as an important reaction by-product. The direct photolysis can be well represented with a six step reaction sequence. The direct ozonation mechanism comprises 22 steps and, with the entire set of kinetic constants completed in this work, it is independent of the reaction pH in the range from 3 to 6.3. Lastly, the associated use of ozone and UVC radiation becomes necessary to consider the existence of radiation absorption by three species, namely DCA, ozone and hydrogen peroxide. The developed system, including the three parallel reactions, led to the proposal of a 37 step reaction mechanism. Finally the reaction kinetics, the mass balances and the radiation field corresponding to this complex system were rigorously modeled and the most significant features of the mathematical representation are briefly described. The simulation results rendered from this model agree very well with the measured experimental data. This outcome will be essential for deriving a complete reactor model that must be appropriate to describe, in the future, the more practical two-phase operating system.

1. Introduction

Haloacetic acids (HAA) together with trihalomethanes (THM) are two of the major chemical families of disinfection by-products (DBP) produced when drinking water has been treated with chlorine.[1] Chlorination is utilized in many countries to generate safe drinking water. Post-chlorination is often the only step implemented after many other water treatment processes. Chlorine reacts with natural organic matter (NOM) not removed completely during treatment to form THMs and HAAs. Numerous investigations have demonstrated that these compounds are associated with the development of cancer, growth retardation, spontaneous abortion and congenital cardiac defects.[2]

Dichloroacetic acid (DCA) is often found as a DPB in disinfected natural water resulting from the combination of free chlorine with humic and other organic substances regularly present. DCA can also be found in wastewaters resulting from the degradation of refuse matter containing chlorinated compounds.[3,4] This substance has been classified as possible carcinogenic compound by the US EPA.[5] On this basis, DCA appears to be an appealing model compound for this study.

Conventional water treatment processes such as air stripping or adsorption by activated carbon are less suitable for DCA, because of its very high solubility in water and very low vapor pressure. In any event, they are not destructive technologies.[6] Thus, advanced oxidation processes (AOP) seem to be an attractive choice to decrease DCA concentrations in polluted waters.

All different forms of ozone-based AOPs possess a high potential for removing pollutants from water sources and from wastewater. In particular the combination of ozone and UV light has proven its effectiveness in removing a wide variety of undesired compounds.[7,8,9]

The reaction of ozone with contaminants in solution is quite complex. In some cases molecules may react directly with ozone, while often simultaneously it may decompose and after a few steps give rise to a very reactive oxidant such as $^{\bullet}OH$ radicals. Ozone can also react through the hydroxyl radical ($^{\bullet}OH$) generated during its decomposition. $^{\bullet}OH$ generation is usually promoted at high pH, with the addition of hydrogen peroxide, UV irradiation or by reaction with the organic compound itself.[10] The hydroxyl radical produces a faster and especially non-selective oxidation with most solutes.[11] Thus, during ozonation in water, both molecular ozone (O_3) and hydroxyl radicals coexist having different reactivity and selectivity. A precise and fundamental study on ozone and

Instituto de Desarrollo Tecnológico para la Industria Química, Universidad Nacional del Litoral and CONICET, CCT Conicet-Santa Fe, Edificio Intec I, Colectora de la Ruta Nacional N° 168, Km. 472.5, (3000), Santa Fe, Argentina. E-mail: mlovato@santafe-conicet.gov.ar; Fax: + 54 (0)342 4511087

† This paper is published as part of the themed issue of contributions from the 6th European Meeting on Solar Chemistry and Photocatalysis: Environmental Applications held in Prague, Czech Republic, June 2010.

hydrogen peroxide decomposition was reported by Lesko *et al.* (2004).[13] This contribution provides very significant insights on the mechanistic aspects of these two processes. Similarly, a valuable, rather new contribution, on the possible mechanism of ozone decomposition in aqueous solutions, was provided by a very intensive study on the existence of reactive intermediates in this reaction. This work was published more recently by Fábián (2006)[14] and provides an updated interpretation of the most important steps, suggesting, particularly, that some of them are almost not detectable and consequently could even be excluded from previous classical proposals.

However, it should be noted that recently[16] it has been found that ozone reaction with natural organic matter leads to peroxide formation. Assuming that the peroxide species generated were mainly hydrogen peroxide, the amount of H_2O_2 generated by the reaction of organic matter with ozone was found to vary with the initial organic load, and to follow a linear dependence on time.

On the other hand, other authors[17] studied the degradation and mineralization of Linuron (*N′*-(3,4-dichlorophenyl)-*N*-methoxy-*N*-methylurea) by O_3 and O_3/UV processes, finding that TOC removal was not possible in sole-UV process, and TOC removal was insignificant in the single ozonation reaction. Using O_3/UV, nearly 80% mineralization was achieved. These results suggested that O_3/UV was a promising process for the final disposal of Linuron.

Degradation of dichloroacetic (DCA) and trichloroacetic (TCA) acids with O_3 alone, UV alone and the hybrid O_3/UV processes were also studied.[4] It was found that single O_3 or UV alone treatments did not result in perceptible decomposition of the haloacetic acids. Advanced oxidation processes, such as O_3/UV or O_3/H_2O_2/UV were effective for DCA degradation. These results confirm that the decomposition of HAAs should be caused by the attack of $^{\bullet}OH$ radicals formed through the photolysis of ozone. The authors also found that the accumulation of H_2O_2 depends on the concentration of organic matter in concordance with Lucas *et al.*[16]

This study was aimed at examining in detail the degradation of DCA by direct photolysis (at 253.7 nm wavelength), ozonation alone without UVC and the O_3/UVC processes in aqueous phase. The effects of different operating variables were investigated and, finally, oxidation byproducts were identified and quantified, in order to develop an operative and, as far as possible, complete reaction scheme based on previous information, our experimental work and plausible reaction paths to explain the gathered results. This is the first step to the proposal of a sound mathematical model for the degradation kinetics of DCA by means of the O_3/UV process employing the more economical semi-batch, two-phase system. However, it must be said in advance that we have found that neither direct photolysis nor direct ozonation are completely negligible reactions. Thus, three parallel reactions are taken into account, as will be shown below.

2. Experimental

2.1. The reacting system

Ozone was produced by an Ozone Generator (Fischer 503), with a nominal input power of 350 W and operating pressure of 0.5 atm. The flow rate of the oxygen inlet gas to the generator was kept at 1.25 mmol s^{-1}. The ozone percentage produced in the gas stream was controlled by changing the power input to the generator. For this work, the generator was operated at three current intensities (50, 100 and 200% of the nominal input power). The rendered concentration of dissolved ozone in aqueous phase was about 1, 1.5 and 2.2×10^{-7} mol cm^{-3} respectively. However, the exact dissolved ozone concentration was measured for every run, finding small differences, as expected, for each experimental determination. The employed photo-reactor was a cylinder made of Teflon™ closed at both ends with two demountable, flat, circular windows made of quartz (Fig. 1). The reactor length was 5.2 cm, and the inner diameter 5.2 cm ($V_{R,irra}$ = 110.4 cm^3), Each window permitted to interpose (i) shutters to block the passage of radiation until the system was at steady state and (ii) neutral density filters to vary the irradiation intensity from the lamps. Irradiation was produced by two tubular germicide lamps placed at the focal axis of their respective parabolic reflectors made of mirror polished aluminium. Three different types of radiation sources were used: (i) two Philips TUV lamps having an input power of 15 W each, (ii) two Heraeus NNI 40/20 operated with an input power of 40 W each (100%) and (iii) two Heraeus NNI 40/20 lamps with neutral density filter (21.6%). These lamps are low pressure mercury lamps, with one single significant emission wavelength at 253.7 nm and no emission below 250 nm.

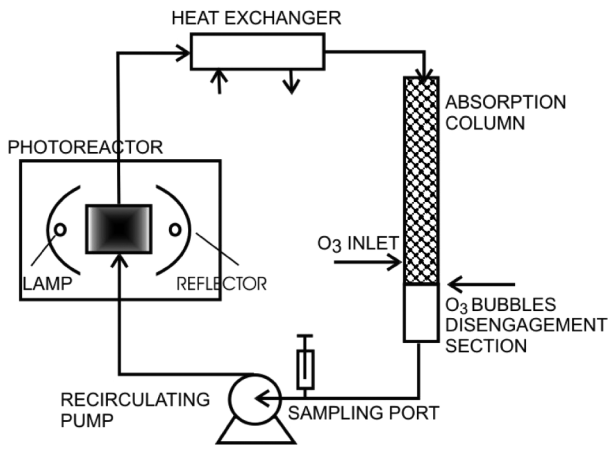

Fig. 1 Schematic representation of the experimental device.

The photo-reactor was part of a recirculating system as follows. (i) An absorption column made of transparent acrylic plastic filled with small Raschig rings. At the top there is the liquid inlet; the fluid flows downward after dispersion through a flow distributor. Ozone circulates countercurrent. The column is divided into two parts by a perforated plate (with very small holes) that serves to support the column packing and allows the motion of the liquid downwards. The gas enters the column above this plate. The special construction of this device impedes the passage of ozone bubbles to the bottom part of the column. (ii) The stream of the output liquid is sent to a stainless steel centrifugal pump (made with Viton® sealings) that feeds the fluid into the photoreactor and recirculates the reaction mixture through the whole system. Under these conditions the photoreactor operates in a homogeneous phase. (iii) A heat exchanger connected to a thermostatic bath to keep the system temperature constant at 20 °C. From experimental measurements, under the employed hydrodynamic conditions, the

volumetric mass transfer coefficient of the mixture oxygen-ozone to water in the packed column was $k_L a = (1.15 \pm 0.1) \times 10^{-2}$ s^{-1}. This value compares satisfactorily with the results published by Lucas *et al.* (2009)[16] and Garoma and Gurol (2005).[15] They reported a value of: $k_L a = 1.12 \times 10^{-2}$ s^{-1} and 8.8×10^{-3} s^{-1} for their experimental setups, respectively.

The total recirculating fluid volume was 1700 cm^3 and the whole equipment is protected from extraneous light.

2.2. Experimental procedure

Each run adhered to the following protocol: the oxygen supply to the ozone generator was turned on and the produced mixture of oxygen and ozone was vented and the germicidal lamps were turned on (during this time the shutters at the reactor windows were on). Then, the solution was prepared at the desired concentration of DCA, and began to recirculate by means of the centrifugal pump through the system to achieve good mixing. This stabilization was carried out at least for 30 min before starting each experience. Once the ozone generator and the lamps were stabilized, before unlocking the passage of radiation to the photoreactor, the gas stream was fed to the column for 15 min, to saturate the liquid phase and stabilize the concentration of ozone in the system. The moment when the shutter was removed was considered the initial time for the runs involving O_3/UVC or UVC alone (without ozone). For the runs without radiation (ozone alone), the reacting system and its operation was different: the zero time was taken when the intake valve of the O_3 absorption column was open, *i.e.*, for experiments employing only ozone, the above mentioned complete saturation of the solution was not sought, because from the moment when the gas entered the liquid phase the reaction with DCA, at the stated measured concentrations, was initiated. Consequently the time $t = 0$ corresponds to the instant when the inlet valve was open. This was not a problem for experiments of degradation of DCA with ozone plus UVC because the reaction of DCA with ozone alone is very slow compared with the one when UVC radiation was also incorporated. The initial reaction pH was 3.5 ± 0.1.

From these moments on, samples were taken at definite time intervals and the concentrations of DCA, Cl^-, H_2O_2 and total organic carbon (TOC) and the pH were analyzed. The usual reproducibility tests in all runs and analytical determinations were practised (triplicated).

It must be noticed that with the employed laboratory setup, those reactions that involve UVC radiation have an average retention time much smaller that the total time for reactions and/or experiments occurring in the total volume, given by the ratio of $V_{R,irra}/V_{Tot} = 6.5 \times 10^{-2}$.

2.3. Analytical methods

The following reactants were used: (a) DCA (Merck, p.a., >99%), (b) indigo potassium trisulfonate (Aldrich), (c) sodium phosphate monobasic (Anhedra, p.a., >99%), (d) potassium chloride (Merck, p.a., >99%).

Analyses were made as follows: DCA and chloride ion were analyzed by ion chromatography (Dionex 2020i) with a conductivity detector employing an Ion Pac AS4A-SC analytical column and a solution of $NaHCO_3$ 1.7 mM/Na_2CO_3 1.8 mM.

Table 1 Experimental program

Variable	Range
DCA initial concentration	0.196–0.455 mM
Ozone dissolved concentration	0.102–0.256 mM
Initial reaction pH	3.5 ± 0.1
Photon fluence rate at the reactor windows × 10^8 (einstein cm^{-2} s^{-1}). For monochromatic radiation the subscript λ may be omitted. ($E_{\lambda,p,0,W}$). See information below in Section 3.	
Lamp Heraeus 40 W (total)	5.37
Lamp Philips 15 W (total)	2.14
Lamp Heraeus 40 W + Neutral Filters (total)	1.16

The concentration of ozone in the aqueous phase was determined spectrophotometrically at 600 nm employing a Cary 100 Bio UV–vis instrument by the indigo blue method.[18] This method is simple, and has the advantage that hydrogen peroxide and organic peroxides do not interfere if the reading is done within the first 6 h.[19] H_2O_2 was not a reactant but a large concentration byproduct of the ozone photolysis. It was analyzed with a spectrophotometric method at 350 nm.[20] This method is based on the oxidation of KI; thus, any oxidant will react with KI. By this method "total oxidants concentration" was measured, and since the determination of ozone was not affected by H_2O_2, subtracting from the previous result, the concentration of H_2O_2 was obtained by difference. Total organic carbon (TOC) was analyzed (Shimadzu TOC-5000A) in order to compare the degradation of DCA with the total degradation rate to have better information concerning possible reaction intermediates. pH was controlled along the reaction using an Altronix digital thermo-pH-meter, provided with a PY-41-Alpha-Altronix pH electrode.

Samples were taken initially every 15 min, and afterwards every 30 min. They were analyzed immediately after they were taken. A normal run lasted for 4 h.

3. Experimental results: analysis and discussion

3.1. Preliminary runs

3.1.1. The photon fluence rate at the reactor walls. Incident radiation at the windows of the photoreactor was evaluated with actinometer measurements using potassium ferrioxalate.[21] The details of the employed equations are given in Appendix I. For the monochromatic lamps utilized in this work (Heraeus NNI 40 W (100%), Philips TUV 15 W, and Heraeus NNI 40 W + neutral filters (21.6%)) the incident (at the wall) photon fluence rates are reported in Table 1. These numbers comprise the sum of the values corresponding to both windows.

Notice that in this particular case employing monochromatic light, the photon fluence rate is equal to the spectral photon fluence rate; thus the subscript λ, as well as nm^{-1} in the units, will be always omitted.

Two groups of controlling runs were made to investigate the eventual effect of UVC radiation alone and ozone alone separately.

3.1.2. The direct photolysis of DCA with UVC without ozone. A series of experiments were made to evaluate direct photolysis of DCA. With an initial concentration of DCA equal to 2.25 × 10^{-7} mol cm^{-3} (29 ppm), recirculation under the normal operating conditions and operating with the lamp of 40 W, DCA conversions,

Table 2 Proposed reaction sequence for DCA photolysis

	Reaction	Reference
(1)	$HCl_2COO^- \xrightarrow{h\nu} {}^{\bullet}CCl_2CO^- + {}^{\bullet}OH$	This work[a]
(2)	$CCl_2HCOO^- + {}^{\bullet}OH \rightarrow {}^{\bullet}CCl_2HCCO^- + H_2O$	Zalazar *et al.* (2007)[24]
(3)	${}^{\bullet}CCl_2HCOO^- + O_2 \rightarrow {}^{\bullet}OOCCl_2COO-$	Zalazar *et al.* (2007)[24]
(4)	$2{}^{\bullet}OOCCl_2COO^- + 2H^+ \rightarrow 2COCl_2 + 2CO_2 + H_2O + \frac{1}{2}O_2$	Zalazar *et al.* (2007)[24]
(5)	${}^{\bullet}CCl_2CO^- + O_2 \rightarrow COCl_2 + CO_2$	Zalazar *et al.* (2007)[24]
(6)	$Cl_2CO + H_2O \rightarrow 2\ HCl$	Zalazar *et al.* (2007)[24]

[a] Suggested by Singleton *et al.* (1999) for acetic acid.

defined as $x = ([DCA]^0 - [DCA])/[DCA^0]$, were 10.5% and 21.8% after 2 and 4 h respectively. Additional runs were made with the lamp of 15 W of nominal input power to confirm the tendency. With these lamps, DCA conversion was 4.7% after 2 hs, and 8.4% after 4 hs. The results are shown in Fig. 2(a). Thus, it can be concluded that direct photolysis is not negligible.

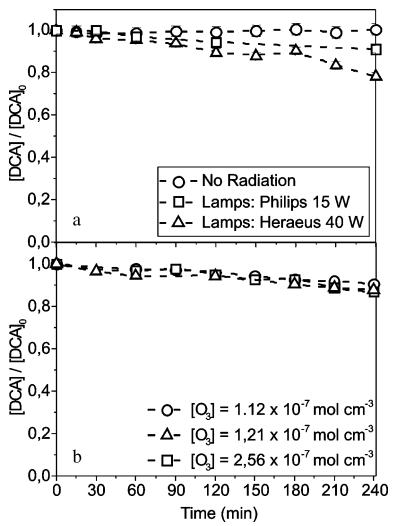

Fig. 2 (a) Direct photolysis (no ozone); (b) direct ozonation (no UVC).

Absorption of UV radiation by DCA starts around 290 nm with very weak values till 250 nm. At 254 nm, $\kappa_\lambda = 3.56 \times 10^4$ cm^2 mol^{-1}. From this point on it begins to increase very sharply to rather high values in the far UV region. However, absorption at 253.7 nm is enough to produce a measurable direct photolysis. Early studies for acetic acid[22] reported that for an assumed wavelength range between 240 and 254 nm, in different proportions several primary products coexist: (1) $CH_4 + CO_2$, (2) $CH_3CO^{\bullet} + {}^{\bullet}OH$, (3) $CH_3^{\bullet} + {}^{\bullet}CPPH$ and (4) $CH_3COO^{\bullet} + H^{\bullet}$. More recently, work on carboxylic acids performed by Singleton *et al.*[23] has shown that at room temperature and up to 222 nm, for the monomeric form of acetic acid, the principal primary product is the formation of the ${}^{\bullet}OH$ radical (about 70%). It is considered that the substitution of two hydrogen atoms in the methyl group by chlorine atoms will reinforce this mechanism for DCA photolysis along this pathway. Once this radical is formed, the reaction follows almost the same track that is already known for the reaction of the radicals ${}^{\bullet}CCl_2COO^-$ and ${}^{\bullet}CCl_2CO^-$ with oxygen as well as the decomposition of ${}^{\bullet}OOCCl_2COO^-$ that leads to the formation of (1) hydrogen chloride (HCl) and (2) phosgene (Cl_2CO) as end reaction products. The last, in the presence of water, decomposes immediately.[6,24] Consequently the photolytic reaction could be explained in terms of the steps shown in Table 2. It can be noted that, as should be expected, in the aqueous system, reaction (6) is very fast and not even traces of $COCl_2$ have been detected as a stable product. In this reaction, under no circumstances were detectable amounts of hydrogen peroxide found. Fig. 2(a) shows the experimental data for DCA concentration as a function of time, the input power of the lamp being the parameter. Initial concentration of DCA was between 2.25 and 2.31×10^{-7} mol cm^{-3} (~30 ppm). Along the reaction, pH varies from 3.6 to 3. Under these conditions it should be noted that the produced carbon dioxide was always under the form of ionized carbonic acid (CO_3^{2-}).

3.1.3. The direct ozonation of DCA without UVC radiation. Three additional sets of runs were made to evaluate direct oxidation of DCA by ozone in the absence of UV radiation. For dissolved ozone, nominal concentrations of 1.12, 1.21 and 2.56×10^{-7} mol cm^{-3}, conversions after 4 h of reaction were 9.3%, 12.1%, and 13.1% respectively.

The same conclusion as before can be drawn and the results are shown in Fig. 2(b). Recall that for each run the actual concentration of ozone has been measured separately. The possibility of an optimum molar concentration ratio of ozone with respect to DCA does not seem to be present. There is consistency with the expected changes. Decomposition of ozone leads to the formation of $HO_2^{\bullet}$ and, after several steps, to the production of the radical ${}^{\bullet}OH$. In any event, the total oxidant concentration remains approximately constant. The concentration of H_2O_2 as an end product was very small. This is in agreement with previous results obtained by Lovato *et al.*[25] for the spontaneous decomposition of ozone.

The mechanistic interpretation of this reaction includes most of the steps reported in Lovato *et al.*,[25] updated with new information and better parameter estimations (valid for the pH range from 3 to 6.3) plus the ones above mentioned reactions in section 3.1.2 for the attack of the ${}^{\bullet}OH$ radical on DCA, in order to complete the process and produce the same end products.[6,25] The observation of small hydrogen peroxide concentrations as an end product, in agreement with the comments in section 3.1.2, are important to compare these results with those that will be analyzed in the main

Table 3 Proposed reaction sequence for DCA ozonation

	Reaction	Reference
(1)	$O_3 + OH^- \rightarrow HO_2^- + O_2$	Tomiyasu *et al.*, 1985[34]
(2)	$O_3 + HO_2^- \rightarrow {}^{\bullet}HO_2 + {}^{\bullet}O_3^-$	Tomiyasu *et al.*, 1985[34]
(3)	${}^{\bullet}HO_2 \rightarrow {}^{\bullet}O_2^- + H^+$	Westerhoff *et al.*, 1997[12]
(4)	${}^{\bullet}O_2^- + H^+ \rightarrow {}^{\bullet}HO_2$	Westerhoff *et al.*, 1997[12]
(5)	$O_3 + {}^{\bullet}O_2^- \rightarrow {}^{\bullet}O_3^- O_2$	Sehested *et al.*, 1983[35]
(6)	${}^{\bullet}O_3^- + H^+ \rightarrow {}^{\bullet}HO_3$	This work
(7)	${}^{\bullet}HO_3 \rightarrow {}^{\bullet}O_3^- + H^+$	This work
(8)	${}^{\bullet}HO_3 \rightarrow {}^{\bullet}OH + O_2$	Bühler *et al.*, 1984[27]
(9)	$O_3 + HO^{\bullet} \rightarrow {}^{\bullet}HO_4$	Lesko *et al.*, 2004[13]
(10)	$CCl_2HCOO^- + {}^{\bullet}OH \rightarrow {}^{\bullet}CCl_2HCOO^- + H_2O$	This work
(11)	${}^{\bullet}CCl_2HCOO^- + O_2 \rightarrow OOCCl_2COO-$	Zalazar *et al.* (2007)[24]
(12)	$2{}^{\bullet}OOCCl_2COO^- + 2H^+ \rightarrow 2COCl_2 + 2CO_2 + H_2O + \frac{1}{2}O_2$	Zalazar *et al.* (2007)[24]
(13)	$Cl_2CO + H_2O \rightarrow CO_2 + 2HCl$	Zalazar *et al.* (2007)[24]
(14)	${}^{\bullet}HO_4 \rightarrow {}^{\bullet}HO_2 + O_2$	Staehelin *et al.*, 1984[36]
(15)	$HO_2^- + H^+ \rightarrow H_2O_2$	Westerhoff *et al.*, 1997[12]
(16)	$H_2O_2 \rightarrow HO_2^- + H^+$	Westerhoff *et al.*, 1997[12]
(17)	${}^{\bullet}HO_4 + {}^{\bullet}HO_4 \rightarrow H_2O_2 + 2O_3$	Staehelin *et al.*, 1984[36]
(18)	${}^{\bullet}HO_4 + {}^{\bullet}HO_3 \rightarrow H_2O_2 + O_2 + O_3$	Staehelin *et al.*, 1984[36]
(19)	${}^{\bullet}OH + H_2O_2 \rightarrow {}^{\bullet}HO_2 + H_2O$	Christensen *et al.*, 1982[37]
(20)	${}^{\bullet}OH + HO_2^- \rightarrow {}^{\bullet}HO_2 + OH^-$	Christensen *et al.*, 1982[37]
(21)	${}^{\bullet}OH + {}^{\bullet}OH \rightarrow H_2O_2$	Buxton *et al.*, 1988[38]
(22)	${}^{\bullet}HO_2 + {}^{\bullet}HO_2 \rightarrow H_2O_2 + O_2$	Bielski *et al.*, 1977[39]

reaction [Fig. 3(a)]. The complete new set of proposed steps is summarized in Table 3.

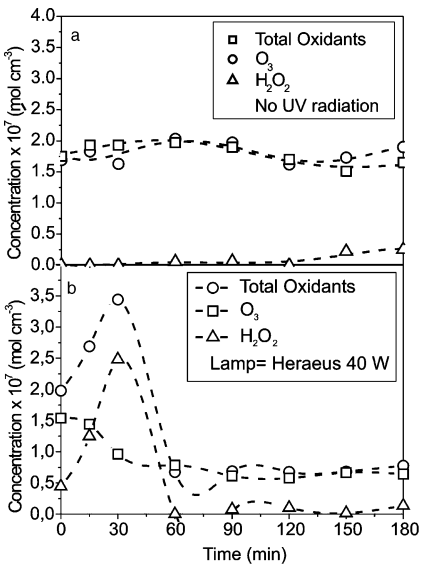

Fig. 3 (a) Total oxidant concentrations in the dark. (b) Total oxidant concentrations in the presence of UVC radiation.

In order to compare the very significant differences existing between these results and the case where there is an external activation, it is interesting to show the effect produced in the system (O_3/H_2O) by the addition of UV radiation (Heraeus NNI 40 W lamp was used here). It was found (see next section) that ozone photolysis leads again to the formation of H_2O_2 but at a much higher rate and exceedingly larger concentrations. The plot presents a maximum in its progression, as seen in Fig. 3(b) (accumulation and subsequent decay). The maximum coincides with a minimum in ozone concentration that is reversed when the concentration of H_2O_2 seems to move upwards to a sort of steady state value. There is a small section in the plot when both the hydrogen peroxide and the ozone start to increase their presence again; also, a decrease in the value of the total oxidant concentration can be observed, consistent with the observed variations of ozone and hydrogen peroxide.

From these results, it can be seen that in the absence of UV radiation there is not significant H_2O_2 formation, while through the combination with UVC radiation, hydrogen peroxide is generated in a considerable amount. This phenomenon is observed in both cases; *i.e.* for 50 and 100% current intensities. The second set is not shown here but the behavior is similar. The only change is the absolute value of measured concentrations given the fact that an increase in the current intensities in the ozone generator renders a greater concentration of ozone, and therefore a greater H_2O_2 production.

3.2. Reaction with ozone and UVC

3.2.1. Effect of ozone concentration. To account for the effect of ozone concentration on the degradation of DCA, several experiments were done over a range of dissolved ozone nominal concentrations of 1.46 to 2.1×10^{-7} mol cm^{-3}.

The same routine was performed for the two lamps that were used in this part of the work (15 W and 40 W). The results are shown in Fig. 4(a) and (b). It can be noted, particularly with the 15 W input power lamp, that the rate of degradation of the pollutant is not greatly affected by a 200% change in the ozone feed concentration. Using 15 W lamps, after 4 h of reaction, for almost all ozone concentrations, 100% conversion was achieved, while for runs with 40 W lamps, for all ozone concentrations, 100% conversion was achieved after 2 h of reaction. However, with a greater input power in the ozone generator and in the lamp, the concentration curves are not so much superposed; *i.e.* changes employing the 40 W lamps are moderately more notorious which is

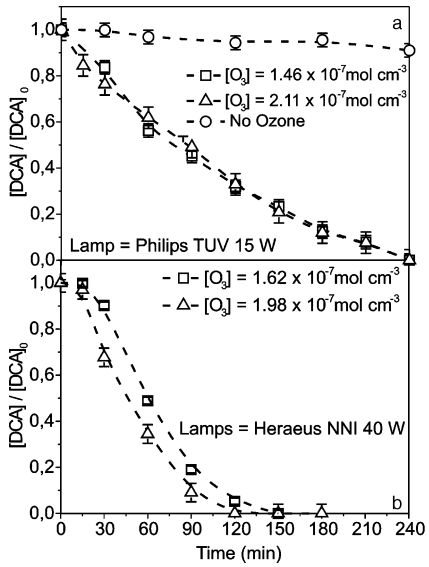

Fig. 4 (a) and (b): Effect of ozone concentration.

an indication of a possible unusual behavior compared with those obtained with 15 W of input power. For low irradiation rates the plot of $[DCA]/[DCA]_0$ *vs.* time did not show significant effects. All the experimental data, regardless of the ozone concentration, fall within a narrow strip that could surely be approximately represented in terms of a pseudo-first order reaction. Also, these results should be analyzed considering the rather large value of the absorption coefficient of ozone. Consider those two runs where DCA initial nominal concentration was 3.10×10^{-7} mol cm^{-3} (40 ppm) and Philips TUV 15 W lamps were utilized (Fig. 4(a)). A possible explanation for this behavior could be that when the 15 W lamp is used, for rather high concentrations of DCA, since the radiation absorption of ozone at 253.7 nm is important, there may be a scant supply of the necessary amount of photons and, regardless the existing ozone concentration, the degradation rates of DCA are approximately similar; *i.e.* the insufficient value of the fluence rate at the reactor entrance produces a controlling effect on the degree of the DCA oxidation rate (see Fig. 4). In effect, if one considers a virtual nominal optical thickness ($\kappa C_{O_3}{}^0 L_R$) based on the initial ozone concentration and the reactor length in the main direction of radiation propagation, for the value of $\kappa = 3.6 \times 10^7$ cm^2 mol^{-1} at 253.7 nm and the fluence rate at the reactor windows $E_{p,o,W}$ for the lamp of nominal input power of 15 W, in a first approximation, most of the incoming photons could be absorbed regardless the value of the selected set of ozone concentrations. Along the same reasoning it is possible to compare these results with the ones shown in Fig. 4(a) and 4(b). In the second case with a the lamp of 40 W input power, the curves are slightly less superposed and can be much better observed the small effect produced by the increase in ozone concentration as discussed before.

3.2.2. Effect of UV photon fluence rate at the reactor windows ($E_{p,o,W}$). Evolution of $[DCA]/[DCA]_0$ under various UVC photon fluence rates at the reactor windows for a DCA initial concentration of 3.1×10^{-7} mol cm^{-3} (40 ppm) are shown in Fig. 5. In all cases, the 100% power input of the ozone generator was used (all measured dissolved ozone concentrations were about

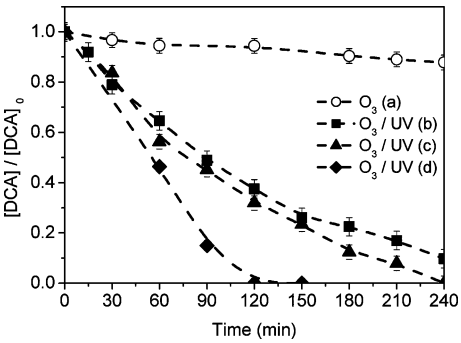

Fig. 5 Effect of incident photon fluence rate at the reactor windows. Average employed ozone concentrations were (a) 1.21, (b) 1.46 (c) 1.39 (d) 1.20×10^{-7} mol cm^{-3}.

1.5×10^{-7} mol cm^{-3}). From this figure, it can be deduced the great influence of the incident photon fluence rate on the degradation of the pollutant. If we take a midway reaction time of 2 h (7200 s), the achieved DCA conversions are 5.57%, 62.51%, 68.05% and 100% for O_3 alone (a) (no UVC), 40 W + filters (b), 15 W (c) and 40 W (d) respectively. However, it must be taken into account that this is only an approximate statement, because the correct evaluation should be made with the photon absorbed radiant power density, also called averaged volumetric rate of photon absorption, as will be shown in section 5. In any event, it can be seen at a glance that the expected non-linear dependence of the rate with respect to this variable is present.

The results shown in Fig. 5 cannot be analyzed with accuracy without a complete modeling of the reaction kinetics, the spatial distribution of the radiation field and the exact evaluation of the absorbed radiant power density (or the local value of the rate of photon absorption). However, some hint about the qualitative expected performance can be induced from the effect produced by the variation of conversion of DCA as a function of the photon fluence rate at the reactor windows. This could be done resorting to the equation of a kinetics following the typical power law function:

$$\left\{1 - \frac{[\mathrm{DCA}]}{[\mathrm{DCA}]_0}\right\} = K\left(E_{p,o,W}\right)^n$$

Upon linearization, an exponent approximately equal to 0.44 is obtained for the different measured values of the experimental data. This is only a very crude indication of the information that could only be properly obtained resorting to a complete kinetic model. It will be the scope of a next section once we define a tentative reaction mechanism for this very complete set of three parallel reactions. In any event it is an acceptable indication that the expected dependence for a homogeneous photochemical reaction lies in the proximities of the most often observed limits (between 0.5 and 1).

3.2.3. Effect of DCA initial concentration. The conversion of DCA at a given time decreases when raising the concentration of pollutant. Three sets of runs were done, with initial DCA concentrations of 20, 40 and 50 ppm (1.55, 3.10 and 3.88×10^{-7} mol cm^{-3}). After 2 h of reaction, the reached conversions are 100%, 97.0% and 90.5% respectively. When all other operating conditions are constant, this is often an anticipated result for most homogeneous reactions. However, this statement does not imply

that the rates are in the same progression, but quite the opposite. In a rapid analysis a pseudo-first order approximation can be used. With data at the following concentrations of DCA: 1.74×10^{-7}, 2.65×10^{-7} and 3.85×10^{-7} mol cm^{-3}, the following average first order constant is 1.92×10^{-4} s^{-1}, with $R^2 = 0.95$. If one accept a pseudo-first order constant equal 1.09, for a 95% confidence interval and $R^2 = 0.999$ all the experimental points are very well represented. However, it must be taken into account that this work has been performed with low concentrations of DCA and this interpretation should not be directly extrapolated to higher ones.

3.2.4. Chloride ion evolution. HCl is one reaction product that can be easily measured. In this work, chloride ion and DCA were measured independently by ion chromatography. If there is complete degradation, then there is a stoichiometric relationship between decomposed DCA and formed chloride ions. For each mole of DCA decomposed, two moles of HCl should be present. Hence, it is possible to compare two values of Cl^- concentration obtained separately: (i) directly measured by ion chromatography, and (ii) calculated from the stoichiometric relationship applied to the concentrations of DCA that were also experimentally assessed but determined separately. Fig. 6(a) shows these results for a typical run. From these data, it can be said that Cl^- ion almost exactly follows the stoichiometric relationship for all times. Thus, it can be concluded that the presence of stable, chlorinated intermediate compounds does not occur at any time during the reaction.

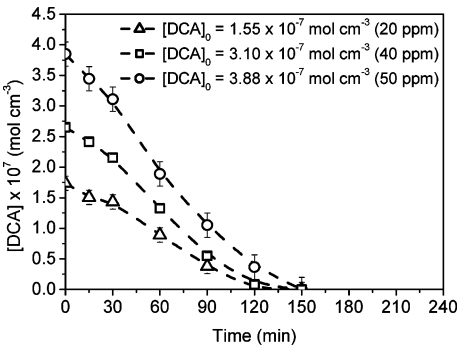

Fig. 6 Effect of the DCA initial concentration.

3.2.5. Total organic carbon (TOC) evolution. Determination of TOC is important to decide if the process is capable of giving complete degradation of the pollutant. Its quantification is important from two view points: (i) if DCA is totally removed and the TOC concentration is zero, it can be definitely concluded, as above, that the process gives complete degradation, and (ii) the TOC theoretical concentration equivalent to the experimentally measured DCA concentration can be calculated and both results readily compared. If there are no stable intermediates along the whole run, these two evolutions must be the same. Fig. 7(b) shows the results for the same run shown in Fig. 7(a). From these results, and from those found for the chloride ion evolution, it can be inferred that in aqueous media DCA degradation by the O_3/UV advanced oxidation process does not generate stable reaction intermediates at any point.

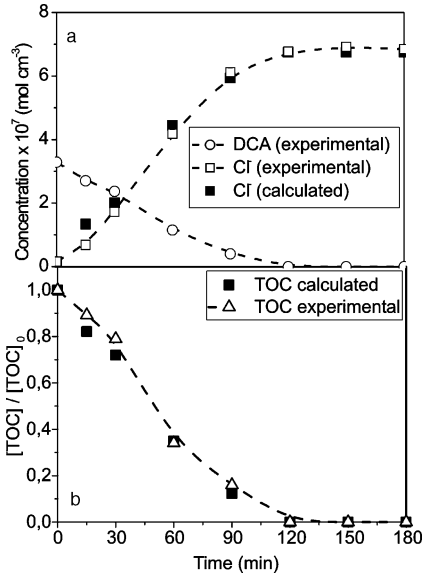

Fig. 7 (a) Comparison of DCA degradation concentration and ion chloride evolution (measured and resulting from the theoretical stoichiometry). (b) Comparison of TOC measured concentration and TOC theoretical equivalent concentration corresponding the DCA measured concentration. $C_{O_3}{}^0 = 1.02 \times 10^{-7}$ mol cm^{-3}, $C_{DCA}{}^0 = 3.29 \times 10^{-7}$ mol cm^{-3}, lamps: Heraeus 40 W.

3.3. H_2O_2 evolution

As shown in previous sections, ozonation of DCA in aqueous phase produces a small amount of hydrogen peroxide as a byproduct. The phenomenon is quite different when the photolysis of ozone takes place. For this reason, in the case of the complete reaction (including both ozone and UVC radiation) it is very important to know the evolution of this byproduct for two main reasons: (a) it is also an oxidant at the employed wavelength and (b) in spite of it having an appreciably smaller molar Napierian absorption coefficient, it competes with ozone for the existing photons in the system. Notwithstanding that the main objective of this research is the DCA decomposition, the hydrogen peroxide generation reaches such high values that a brief discussion concerning the effects of the main experimental variables influencing its production seems appropriate.

3.3.1. DCA initial concentration. For each performed run, H_2O_2 concentration was measured as described in the Experimental section. Its evolution presents an important accumulation followed by a slight diminution in the increasing rate of formation. This is even more noticeable in the case of the lower DCA concentration, implying the possible existence of a maximum for all cases. For these three runs the current intensity in the generator was 100% and Philips TUV 15 W lamps were utilized. The higher the concentration of pollutant, the higher the increase in H_2O_2 concentration that is produced. These results agree with the observations existing in the literature.[4,17,26] Also, it may be thought that for smaller DCA initial concentrations the curve of total oxidants goes to a maximum. This result could be interpreted as evidence that when the concentration of DCA falls to very low values, the hydroxyl radicals generated in the decomposition of ozone do not have enough pollutant to react with and, as an alternative, attack H_2O_2, which generates its corresponding

concentration decrease (the well-known scavenging effect of •OH radicals on H_2O_2). This observation is in accordance with the time when the maximum hydrogen peroxide concentration is measured, which appears earlier than the moment when the pollutant concentration becomes lower, as can be observed in Fig. 8.

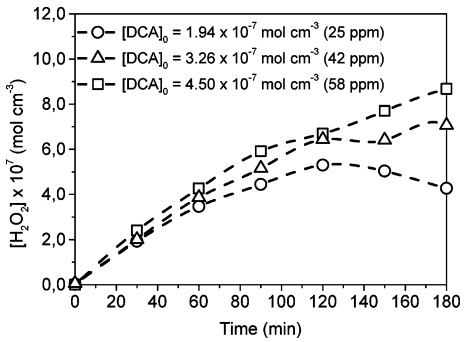

Fig. 8 Effect of DCA concentration on hydrogen peroxide concentration.

3.3.2. Effect of ozone concentration on the hydrogen peroxide formation. As can be seen in Fig. 9, when the contaminant is degraded, the formation of hydrogen peroxide is not greatly affected by changes in the dissolved concentration of ozone, which is different from the observed behavior in the system (O_3/H_2O). In fact, in this case, one could have thought that the production of H_2O_2 should have been enhanced by the increasing ozone concentration in the liquid phase. This is not the case. This result could be an indication that probably the intensification of the concentration appearance of hydrogen peroxide is, additionally, very much related to the existence of an important reaction intermediary, a particular radical, which is formed when DCA is present.

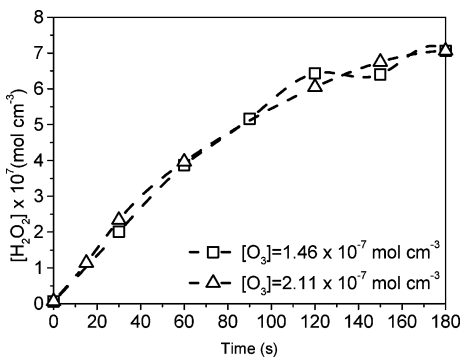

Fig. 9 Effect of ozone concentration on hydrogen peroxide formation.

From the previous information concerning DCA ozonation, it is possible to postulate that probably, the presence of the $^{\bullet}OOCCl_2COO^-$ radical accompanied by ozone is critical in this reaction. In the next section this problem will be discussed with additional information.

3.3.3. Photon fluence rate at the reactor wall (incident radiation at the wall). When the radiation intensity is increased, the maximum concentration of H_2O_2 is reached earlier, as shown in Fig. 10. In these cases, DCA initial concentration was 3.30 and 2.65×10^{-7} mol cm^{-3} (40 ppm approximately) for experiments with

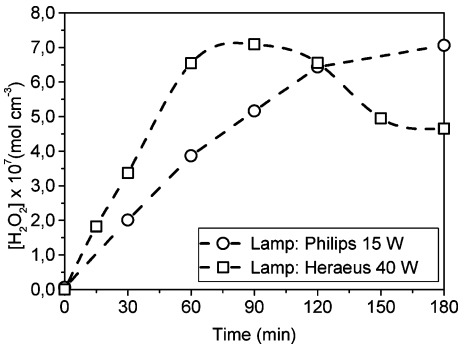

Fig. 10 Effect of the photon fluence rate on the H_2O_2 formation.

15 W and 40 W Lamps respectively. The ozone generator current intensity was 100%.

Notice in Fig. 5 that when the 40 W lamps are used the degradation rate of DCA is much higher. As shown in Fig. 3, the addition of UVC radiation to the system (O_3/H_2O) leads to H_2O_2 formation. Then, the consequence of an increase in the photofluence rate at the reactor windows will be an increase in the hydrogen peroxide formation. This phenomenon happens before the own decomposition of hydrogen peroxide produces an even higher concentration of •OH radicals that may act as scavengers of the existing oxidant. The shape of the plot for the 15 W lamps may be an indication that the maximum has not been achieved yet.

4. A proposal of a degradation reaction scheme

The decomposition of aqueous ozone in pure water is initiated by its reaction with hydroxide ion (OH^-), and this reaction leads to the production of different radicals that propagate the decomposition process by radical chain reactions and produce hydroxyl radicals (•OH). Also, the photolysis of DCA leads to the formation of •OH radicals. Thus, with differing importance, there are two sources of such a strong oxidant. In a previous work, a reaction kinetic model for ozone decomposition in aqueous media has been proposed and verified.[25] These results have been perfected in this work. The main change corresponds to reactions (9) and (10) on account of the new reported value (erratum publication by Buhler *et al.*)[27] for the pK_a of $HO_3^{\bullet}$, and reaction (12) considering the value reported by Lesko *et al.* (2004)[13] (Table 4). Ozone decomposition is known to occur slowly and could be accelerated working at high pH, or with the addition of hydrogen peroxide or with the enhancement produced by ultraviolet radiation. In the aqueous phase, ozone photolysis produces hydrogen peroxide as a primary product, which then may directly photolyze into hydroxyl radicals.

In this work, ozone, H_2O_2, DCA and Cl^- concentrations have been measured. It was found that chloride evolution agrees with the expected growth calculated from the stoichiometric relationship with DCA degradation. When UV light is incorporated to the system, the development of H_2O_2 concentration increases reaching a maximum value and then decreases to an almost stationary – but high – value.

Based on previous reports[6,13,15,24,25,28,29,30] and our own work here, a tentative kinetic mechanism for DCA degradation was developed. It must be noted that, with the exception of Lovato *et al.*[25] (who used ozone alone and neither DCA nor UVC),

Table 4 Tentative complete reaction mechanism

	Reaction	Kinetic constant value	Reference
(1)	$CHCl_2COO^- \xrightarrow{h\nu} {}^{\bullet}CCl_2CO^- + {}^{\bullet}OH$	$\Phi_{p,DCA} = 0.226$	This work
(2)	$O_3 + H_2O \xrightarrow{h\nu} H_2O_2 + O_2$	$\Phi_{p,O_3} = 0.50$	Gurol and Akata, 1996[40]
(3)	$H_2O_2 \xrightarrow{h\nu} 2\,{}^{\bullet}OH$	$\Phi_{p,H_2O_2} = 0.48$	Baxendale and Wilson, 1957[41]
(4)	$O_3 + OH^- \rightarrow HO_2^- + O_2$	$k_4 = 7 \times 10^4$ cm^3 mol^{-1} s^{-1}	Tomiyasu *et al.*, 1985[34]
(5)	$O_3 + HO_2^- \rightarrow {}^{\bullet}HO_2 + {}^{\bullet}O_3^-$	$k_5 = 2.2 \times 10^9$ cm^3 mol^{-1} s^{-1}	Tomiyasu *et al.*, 1985[34]
(6)	${}^{\bullet}HO_2 \rightarrow {}^{\bullet}O_2^- + H^+$	$k_6 = 7.9 \times 10^5$ s^{-1}	Westerhoff *et al.*, 1997[12]
(7)	${}^{\bullet}O_2^- + H^+ \rightarrow {}^{\bullet}HO_2$	$k_7 = 5 \times 10^{13}$ cm^3 mol^{-1} s^{-1}	Westerhoff *et al.*, 1997[12]
(8)	$O_3 + {}^{\bullet}O_2^- \rightarrow {}^{\bullet}O_3^- + O_2$	$k_8 = (1.6 \pm 0.2) \times 10^{12}$ cm^3 mol^{-1} s^{-1}	Sehested *et al.*, 1983[35]
(9)	${}^{\bullet}O_3^- + H^+ \rightarrow {}^{\bullet}HO_3$	$k_9 = (1.09 \pm 0.49) \times 10^{14}$ cm^3 mol^{-1} s^{-1}	This work
(10)	${}^{\bullet}HO_3 \rightarrow {}^{\bullet}O_3^- + H^+$	$k_{10} = (2.65 \pm 0.64) \times 10^4$ s^{-1}	This work
(11)	${}^{\bullet}HO_3 \rightarrow {}^{\bullet}HO + O_2$	$k_{11} = (1.009 \pm 0.06) \times 10^8$ cm^3 mol^{-1} s^{-1}	Bühler *et al.*, 1984[27]
(12)	$O_3 + {}^{\bullet}OH \rightarrow {}^{\bullet}HO_4$	$k_{12} = 1.1 \times 10^{11}$ cm^3 mol^{-1} s^{-1}	Lesko *et al.*, 2004[13]
(13)	${}^{\bullet}HO_4 \rightarrow {}^{\bullet}HO_2 + O_2$	$k_{13} = (2.8 \pm 0.3) \times 10^7$ cm^3 mol^{-1} s^{-1}	Staehelin *et al.*, 1984[36]
(14)	$HO_2^- + H^+ \rightarrow H_2O_2$	$k_{14} = 5 \times 10^{13}$ cm^3 mol^{-1} s^{-1}	Westerhoff *et al.*, 1997[12]
(15)	$H_2O_2 \rightarrow HO_2^- + H^+$	$k_{15} = 0.125$ s^{-1}	Westerhoff *et al.*, 1997[12]
(16)	${}^{\bullet}HO_4 + {}^{\bullet}HO_4 \rightarrow H_2O_2 + 2\,O_3$	$k_{16} = 5 \times 10^{12}$ cm^3 mol^{-1} s^{-1}	Staehelin *et al.*, 1984[36]
(17)	${}^{\bullet}HO_4 + {}^{\bullet}HO_3 \rightarrow H_2O_2 + O_2 + O_3$	$k_{17} = 5 \times 10^{12}$ cm^3 mol^{-1} s^{-1}	Staehelin *et al.*, 1984[36]
(18)	${}^{\bullet}OH + H_2O_2 \rightarrow HO_2^{\bullet} + H_2O$	$k_{18} = 2.7 \times 10^{10}$ cm^3 mol^{-1} s^{-1}	Christensen *et al.*, 1982[37]
(19)	${}^{\bullet}OH + HO_2^- \rightarrow {}^{\bullet}HO_2 + OH^-$	$k_{19} = 7.5 \times 10^{12}$ cm^3 mol^{-1} s^{-1}	Christensen *et al.*, 1982[37]
(20)	${}^{\bullet}OH + {}^{\bullet}OH \rightarrow H_2O_2$	$k_{20} = 5.2 \times 10^{12}$ cm^3 mol^{-1} s^{-1}	Buxton *et al.*, 1988[38]
(21)	${}^{\bullet}HO_2 + {}^{\bullet}HO_2 \rightarrow H_2O_2\,O_2$	$k_{21} = 8.3 \times 10^8$ cm^3 mol^{-1} s^{-1}	Bielski *et al.*, 1977[39]
(22)	${}^{\bullet}CCl_2HCOO^- + HO^{\bullet} \rightarrow {}^{\bullet}CCl_2COO^- + H_2O$	$k_{22} = (3.4 \pm 0.3) \times 10^{10}$ cm^3 mol^{-1} s^{-1}	This work
(23)	${}^{\bullet}CCl_2COO^- \rightarrow {}^{\bullet}OOCCl_2COO^-$	k_{23}[a]	Zalazar *et al.*, 2007[24]
(24)	$2\,{}^{\bullet}OOCCl_2COO^- + 2H^+ \rightarrow 2COCl_2 + 2CO_2 + H_2O + \frac{1}{2}O_2$	k_{24}[a]	Zalazar *et al.*, 2007[24]
(25)	$COCl_2 + H_2O \rightarrow CO_2 + 2HCl$	k_{25}[a]	Zalazar *et al.*, 2007[24]
(26)	${}^{\bullet}OH + {}^{\bullet}HO_2 \rightarrow H_2O + O_2$	$k_{26} = 6.6 \times 10^{12}$ cm^3 mol^{-1} s^{-1}	Buxton *et al.*, 1988[38]
(27)	${}^{\bullet}OH + {}^{\bullet}O_3^- \rightarrow {}^{\bullet}HO_2 + {}^{\bullet}O_2^-$	$k_{27} = 8.5 \times 10^{12}$ cm^3 mol^{-1} s^{-1}	Sehested *et al.*, 1983[35]
(28)	${}^{\bullet}O_2^- + {}^{\bullet}HO_2 + H_2O \rightarrow H_2O + O_2 + OH^-$	$k_{28} = 9.7 \times 10^{10}$ cm^3 mol^{-1} s^{-1}	Sehested *et al.*, 1984[35]
(29)	${}^{\bullet}OH + {}^{\bullet}O_2^- \rightarrow O_2 + OH^-$	$k_{29} = 9.4 \times 10^{12}$ cm^3 mol^{-1} s^{-1}	Bielski *et al.*, 1977[39]
(30)	$O_3 + H_2O_2 \rightarrow {}^{\bullet}HO_2 + {}^{\bullet}OH^{\bullet} + O_2$	$k_{30} = 1 \times 10^2$ cm^3 mol^{-1} s^{-1}	Staehelin *et al.*, 1984[36]
(31)	$O_3 + HO_2^- \rightarrow {}^{\bullet}O_2^- + {}^{\bullet}OH + O_2$	$k_{31} = 5.5 \times 10^9$ cm^3 mol^{-1} s^{-1}	Staehelin *et al.*, 1984[36]
(32)	${}^{\bullet}HO_2 + {}^{\bullet}HO_4 \rightarrow O_2 + O_3 + H_2O$	$k_{32} = 1 \times 10^{13}$ cm^3 mol^{-1} s^{-1}	Rivas *et al.*, 2006[29]
(33)	${}^{\bullet}OH + {}^{\bullet}HO_3 \rightarrow O_2 + H_2O_2$	$k_{33} = 5 \times 10^{12}$ cm^3 mol^{-1} s^{-1}	Rivas *et al.*, 2006[29]
(34)	${}^{\bullet}HO_3 + {}^{\bullet}HO_3 \rightarrow 2O_2 + H_2O_2$	$k_{34} = 5 \times 10^{12}$ cm^3 mol^{-1} s^{-1}	Rivas *et al.*, 2006[29]
(35)	${}^{\bullet}HO_3 + {}^{\bullet}O_2^- \rightarrow 2O_2 + OH^-$	$k_{35} = 1 \times 10^{13}$ cm^3 mol^{-1} s^{-1}	Rivas *et al.*, 2006[29]
(36)	${}^{\bullet}HO_4 + {}^{\bullet}OH \rightarrow O_3 + H_2O_2$	$k_{36} = 5 \times 10^{12}$ cm^3 mol^{-1} s^{-1}	Rivas *et al.*, 2006[29]
(37)	${}^{\bullet}HO_4 + {}^{\bullet}O_2^- \rightarrow O_3 + O_2 + OH^-$	$k_{37} = 1 \times 10^{13}$ cm^3 mol^{-1} s$^-$	Rivas *et al.*, 2006[29]

[a] In Zalazar *et al.* (2007),[24] these three constants were grouped into a single parameter. The individual values are not known. However, there were not required for the development of the complete set of ODE corresponding to the kinetic model presented in this work.

none of the other contributions report reactions of DCA with ozone. They correspond to similar families of compounds where either DCA or ozone has been used, but reacting separately with other chemical species. The present scheme considers different phenomena that describe the pollutant oxidation: ozone spontaneous decomposition in water, three photochemical reactions (interaction of photons with DCA, O_3 and H_2O_2), several specific DCA degradation reactions (known from oxidations with hydrogen peroxide or titanium dioxide) and several radical–radical termination reactions[29] (many of them proposed in the existing literature for different chemical reactions involving ozone or a very large number of classical publications related to reactions with hydrogen peroxide).

In actual terms, we are dealing with three parallel processes: (1) the direct photolysis of DCA (accounting for 0–20% of the decomposition), (2) the direct ozonation (involving a change in the order of 0–13% in DCA concentration) and (3) the ozone + UVC radiation reaction that leads to a complete degradation, rendering CO_2 (actually in the form of ionized carbonic acid), HCl and H_2O_2. In this proposal we have considered the three contributions.

A remarkable outcome is the larger hydrogen peroxide production. This result forced us to search for the origin of this denouement. The results show that it only happens when both ozone and UVC radiation are working together. But an additional component may affect its generation: the concentration of the employed pollutant (DCA in our case) that facilitates the required reaction steps.

Notice that the kinetic scheme for ozone decomposition in aqueous media was validated in our previous work[25] (and perfected with three changes in this one) and this set of steps can be used to predict with accuracy the evolution of DCA, O_3, CO_2 and HCl. At this point, it should be specially noted that the proposed termination

reactions are essential to explain the experimentally measured hydrogen peroxide concentrations along the whole reaction path. Finally, additional decomposition increments resulting from DCA photolysis and the DCA direct ozonation were experimentally verified in this research.

On this basis, in Table 4 the tentative reaction mechanism is proposed. In this scheme we can distinguish five parts: (i) reaction (1) that represents the primary step of the DCA photolysis, (ii) reactions (2) and (3) are two additional photochemical reactions (the photolysis of ozone and hydrogen peroxide), (iii) reactions (4) to (21) represents the kinetic scheme for the decomposition of ozone in water, (iv) reactions (22) to (25) describe DCA degradation by the hydroxyl radical and (v) reactions (26) to (37) are termination and radical–radical recombination reactions.

By looking at the proposed reaction steps, it can be seen that for each mole of decomposed DCA, two moles of HCl are formed. The only quasi-stable product (phosgene) is rapidly hydrolyzed to complete the degradation process. This is in concordance with the experimental results found in this work.

With these results, it is possible to formulate a mathematical kinetic model which should able to describe DCA oxidation by the O_3/UV advanced oxidation process. This model would be able to theoretically predict the degradation of this pollutant and the evolution of its byproducts. That constitutes the objective of our next work, in order to move to a two-phase system and optimize the ozone consumption.

5. Reactor model

5.1. Mass balance

Our reactor functions inside a recycling system. If the following operating conditions are fulfilled: (i) the whole system operates under well-stirred conditions, (ii) the ratio $V_{R,irra}/V_{Tot} < 1$ (even better when it is $\ll 1$) and (iii) the recirculating flow rate is high such as to have differential conversion per pass in the photoreactor and, at the same time, improve mixing, it can be shown that:[31]

$$\left(\frac{dC_i(t)}{dt}\right)_{Tank} = \left(\frac{V_{R,irra}}{V_{Tot}}\right)\left\langle R_{i,irra}(x,t)\right\rangle_{V_{R,irra}} + \left(\frac{V_{Tot}-V_{R,irra}}{V_{Tot}}\right)R_{i,dark}(t) \quad (1)$$

Eqn (1) describes the variation of composition of the "i" species, which take place in the two different parts of the reacting system, *i.e.* irradiated and dark reactor zones, respectively. The first term of eqn (1) represents the complete set of reactions corresponding to the whole system that are taking place in the irradiated volume (photochemical and thermal steps), and the second term represents the reactions having steps occurring only in the dark volume (thermal reactions).

In our case, for our perfectly mixed reactor, both types of reaction steps participating in the mass balance, "irradiated reactions" and "dark reactions", are described by the mass action law. The photochemical reaction can be thought as the interaction of a chemical species with and immaterial one, having no mass and only energy, represented by the photon.

For a reactive species that participate in dark reactions only, $V_{R,irr} = 0$ and for a reactive species that only result from photochemical activation $V_{R,irr} = V_{Tot}$. In our system, DCA, hydrogen peroxide and ozone take part in both dark and irradiated steps, according to their respective characteristics. In what follows, three typical mass balances are illustrated.

$$\frac{dC_{O_3}}{dt} = \left(\frac{V_{R,irra}}{V_{Tot}}\right)\left\langle R_{O_3}(\Phi_{O_3}e^{a}_{\lambda,O_3}(x,t),C_i,k_j)\right\rangle_{V_{R,irra}} + \left(\frac{V_{Tot}-V_{R,irra}}{V_{Tot}}\right)R_{dark}(C_i,k_j) \quad (2)$$

$$\frac{dC_{H_2O_2}}{dt} = \left(\frac{V_{R,irra}}{V_{Tot}}\right)\left\langle R_{H_2O_2}(\Phi_{H_2O_2}e^{a}_{\lambda,H_2O_2}(x,t),C_i,k_j)\right\rangle_{V_{R,irra}} + \left(\frac{V_{Tot}-V_{R,irra}}{V_{Tot}}\right)R_{dark}(C_i,k_j) \quad (3)$$

$$\frac{dC_{DCA}}{dt} = \left(\frac{V_{R,irra}}{V_{Tot}}\right)\left\langle R_{DCA}(\Phi_{DCA}e^{a}_{\lambda,DCA}(x,t),C_i,k_j)\right\rangle_{V_{R,irra}} + \left(\frac{V_{Tot}-V_{R,irra}}{V_{Tot}}\right)R_{dark}(C_i,k_j) \quad (4)$$

In these equations, $\langle \ldots \rangle$ represents the volume averaging integral, C_i represents the concentration of the "i" species present in the reacting system, k_j represents the kinetic constant for the "j^{th}" reaction step, and $e_\lambda{}^a(x,t)$ is the spectral photon radiation absorption power density, also called spectral local volumetric of photon absorption (LVRPA).

5.2. Radiation balance

For the one-dimensional radiation field that is applicable to our experimental device and monochromatic radiation, the equation for the spectral photon fluence rate at the reactor wall takes the following form (recall that since monochromatic radiation is used, the subscript λ may be dropped):

$$\frac{dE_{p,o}(z,t)}{dz} + \alpha(z,t)\times E_{p,o}(z,t) = 0 \quad (5)$$

Boundary conditions. In the case of this reactor configuration the radiation originating from lamp 1 and 2 may arrive at any point "p" from the two opposite sides. Then:

$$E_{p,o,Tot}(z,t) = E_{p,o,z,I} + E_{p,o,z,II} \quad (6)$$

with:

$$E_{p,o,z,Tot} = E_{p,o,W,I}\exp[-\alpha_{Tot}(t)z] \quad (7)$$

$$E_{p,o,z,II} = E_{p,o,W,II}\exp[-\alpha_{Tot}(t)(L_R - z)] \quad (8)$$

where $E_{p,o,W,I}$ or $E_{p,o,W,II}$ are the photon fluence rates at the wall of the reactor windows and α_{Tot} is the total absorption coefficient of the reacting system (all radiation absorption species, including those not taking part in the reaction).

Incident radiation at $x = 0$ and $x = L_R$ was evaluated with actinometer measurements using potassium ferrioxalate as indicated in Appendix I:

$$\left\langle R^{act}(x,t)\right\rangle_{L_R} = \Phi^{act}\left\langle e^{a}_{act}\right\rangle_{L_R} \quad (9)$$

In eqn (9) the reactant is Fe^{+3}, the reaction product is Fe^{+2} and Φ^{act} is the overall actinometer quantum yield in terms of the product.

In the described reactor, for low reactant conversion, the plot of (Fe^{+2}) *vs.* time gives a straight line. The slope of such straight line at $t \rightarrow 0$ is:

$$E_{p,o,W} = \lim_{t\to 0}\left[\frac{C_{Fe^{2+}} - C^0_{Fe^{2+}}}{t - t^0}\right]_{Tk} \frac{V_{Tot}}{A_R \Phi^{act}} \quad (10)$$

$C_{Fe^{3+}}$, $C_{Fe^{2+}}{}^0$ and t are measured and V_{tot}, A_R and $\Phi_\lambda{}^{act}$ are known. Thus eqn (10) gives the value of the spectral fluence rate at the reactor windows. In Appendix I the method employed for their determination is described in detail.

The local volumetric rate of photon absorption (or the absorbed radiant power density) by the radiation absorption species, at a given point in the reactor (the LVRPA) is given as follows:

$$e^a(z,t) = \alpha_i E_{p,o,z,Tot}(z,t) \quad (11)$$

where α_i is the volumetric absorption coefficient of the (i) species. In our reacting system, $E_{p,o,W,I} = E_{p,o,W,II} = E_{p,o,W}$, then:

$$E_{p,o,z,Tot} = E_{p,o,W}\exp[-\alpha_{Tot}(t)z] + E_{p,o,W}\exp[-\alpha_{Tot}(t)(L_R - z)] \quad (12)$$

Finally, eqn (11) can be expressed as

$$e_i{}^a(z,t) = \alpha_i E_{p,o,W}\{\exp[-\alpha_{Tot}(t)z] + \exp[-\alpha_{Tot}(t)(L_R - z)]\} \quad (13)$$

Eqn (13) describes the local value for e^a. It is necessary to calculate the average value for this property (integration over the reactor volume):

$$\left\langle e_i^a \right\rangle_{L_R} = \frac{2\alpha_i E_{p,o,W}}{\alpha_{Tot} L_R}\left\{1 - \exp\left[-\alpha_{Tot} \times L_R\right]\right\} \quad (14)$$

In our reacting system, there are three absorbing species at 253.7 nm (ozone, hydrogen peroxide and DCA). DCA absorption (3.56 M^{-1} cm^{-1}) (spectroscopically measured) is much smaller than ozone (3600 M^{-1} cm^{-1})[32] and hydrogen peroxide (19.6 M^{-1} cm^{-1}).[32] Thus, we can describe eqn (14) for ozone and hydrogen peroxide as:

$$\left\langle e^a_{O_3} \right\rangle = \frac{2\left(C_{O_3}\kappa_{O_3}\right)E_{p,o,w}}{\left(C_{O_3}\kappa_{O_3} + C_{H_2O_2}\kappa_{H_2O_2}\right)L_R} \left\{1 - \exp\left[-\left(C_{O_3}\kappa_{O_3} + C_{H_2O_2}\kappa_{H_2O_2}\right)\times L_R\right]\right\} \quad (15)$$

$$\left\langle e^a_{H_2O_2} \right\rangle = \frac{2\left(C_{H_2O_2}\kappa_{H_2O_2}\right)E_{p,o,W}}{\left(C_{O_3}\kappa_{O_3} + C_{H_2O_2}\kappa_{H_2O_2}\right)L_R} \left\{1 - \exp\left[-\left(C_{O_3}\kappa_{O_3} + C_{H_2O_2}\kappa_{H_2O_2}\right)\times L_R\right]\right\} \quad (16)$$

6. Comparison of simulations and experimental results

6.1. Results with DCA concentrations

The degradation rate of DCA is very well represented for the model that comprises the three proposed parallel reactions. Fig. 11 shows the results for the following experimental conditions: 100% current intensity of the generator ($[O_3]$ ~ 0.165 mM), lamps Heraeus 40 W, and DCA initial concentration of 0.175 and 0.385 mM.

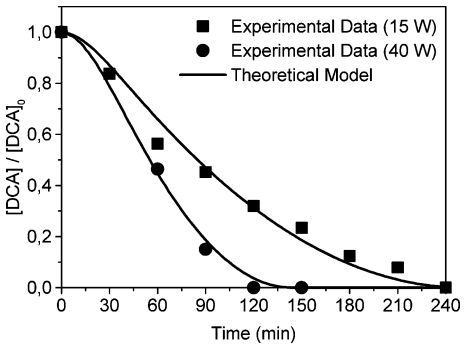

Fig. 11 Theoretical model *vs.* experimental data. Influence of the initial concentration of DCA.

6.2. Results with different absorbed photon flux densities

As shown in Fig. 12, the model provides an excellent concordance with the experimental data measured under the following experimental conditions: 100% current intensities at the ozone generator ($[O_3] \approx 0.130$ mM), DCA initial concentrations of 0.265 and 0.330 mM (40 ppm approx. for both cases), and 40 W and 15 W lamps.

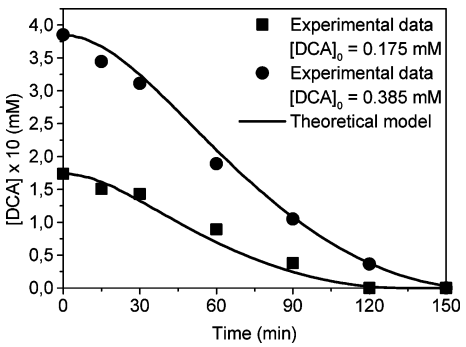

Fig. 12 Theoretical model *vs.* experimental data. Influence of the photo fluence rate at the reactor windows.

6.3. Direct photolyis of DCA

Fig. 13 shows the effect of UV photon fluence rate at the reactor windows ($E_{p,o,W}$) on DCA photolysis. Using the calculated value for ϕ_{DCA}, the theoretical model predicts accurately the experimental data for all cases (15 W lamps, 40 W lamps and a blank run without UV radiation or ozone.

6.4. Correspondence of DCA degradation and formation of chloride concentrations

HCl is one reaction product that can be easily measured. The kinetic model predicts that, for complete degradation, 2 mol of HCl must be formed for each mol of DCA that decomposes.

The complete kinetic model is able to predict this, and in Fig. 14 it can be observed for a typical run, that theoretical simulations

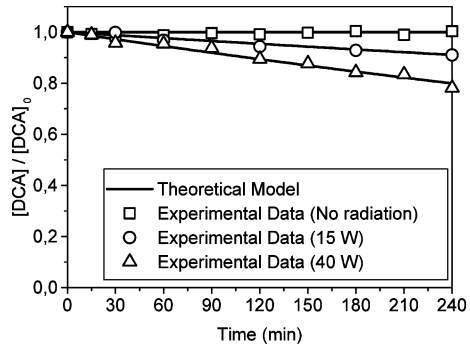

Fig. 13 Theoretical model *vs.* experimental data. DCA photolysis.

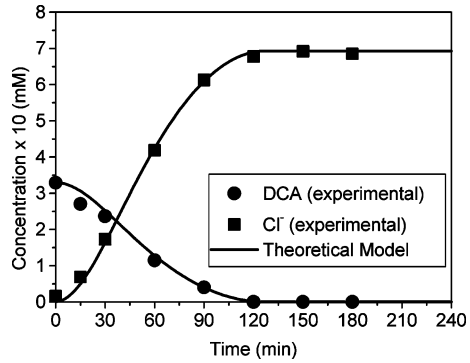

Fig. 14 Theoretical model *vs.* experimental data. DCA and chloride ion evolution.

agree with the experimental data. $[DCA]_0$ = 0.329 mM, $[O_3]$ = 0.1 mM, incident fluence rate = 5.37×10^{-8} einstein cm^{-2} s^{-1}

6.5. Concentration of hydrogen peroxide byproduct

H_2O_2 formed in O_3 photolysis was measured and, comparing the theoretical simulations with the measured concentrations, it can be concluded that the model is able to predict the evolution of all the above mentioned species.

Fig. 15 shows H_2O_2 evolution for the same experimental run described in the previous one.

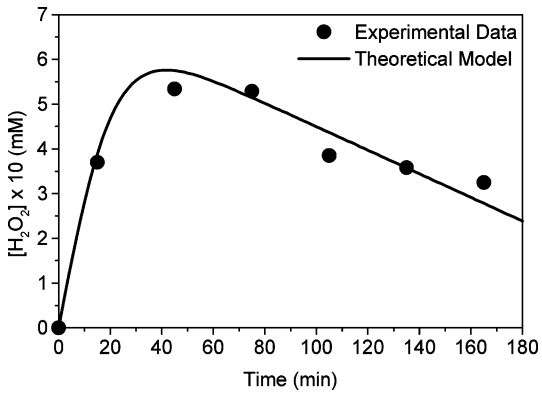

Fig. 15 Theoretical model *vs.* experimental data. H_2O_2 evolution.

It is clear from these five comparisons of computer simulations with experimental data, that the model predictions show very good agreement with the exception of the last portion of the hydrogen peroxide by product formation. Very likely, additional termination steps may be missing. In any event, for such a complex reaction, these results are very satisfactory and constitute a positive and adequate validation of the proposed reaction scheme. This is even more noticeable if it is considered that constitutes the interactive and complementary representation of three parallel reactions contributing to the degradation of DCA under the reported operating conditions.

7. Conclusions

The dichloroacetic acid degradation with advanced oxidation technologies has been studied. The principal conclusions can be summarized as follows:

(I) The influence of various parameters, such as pollutant initial concentration, radiation photon fluence rate at the reactor window and ozone dissolved concentration were studied.

(II) O_3 or UVC by themselves did not result in appreciable decomposition of DCA within the studied reaction time. Conversely, the O_3/UV combination can be considered a suitable process for degrading DCA in water.

(III) It was found that the decomposition of DCA seems to obey a pseudo-first order kinetics with respect to its initial concentration, that the incident photon fluence rate is a very important parameter, affecting in significant manner the reaction rate and that dissolved ozone concentration did not influence appreciably the DCA degradation.

(IV) The evolution of chloride ion and H_2O_2 were permanently measured. Complete DCA removal was achieved, and the mass balance, considering DCA disappearance and chloride ion formation closed within very small error. Consequently it was found that in aqueous media there are no stable intermediaries at any moment of the reaction evolution.

(V) The combination of ozone and UVC radiation produces a significant amount of hydrogen peroxide as an important reaction by-product.

(VI) The kinetics includes the combination of three parallel reactions: (1) direct photolysis, (2) direct ozonation and (3) ozone + UVC degradation.

(VII) The direct photolysis can be well represented with a six step reaction sequence having a primary quantum yield equal to 0.226. The direct ozonation mechanism comprises 22 steps and, with the entire set of kinetic constants complemented in this work, it is independent of the reaction pH in the range from 3 to 6.3. Lastly, in the associated use of ozone and UVC radiation, it is necessary to consider the existence of radiation absorption by three species, namely DCA, ozone and hydrogen peroxide.

(VIII) Based on our results and additional information existing in the literature, a mechanism consisting of 37 steps was derived for the proposed compounded three parallel reactions.

(IX) With this background, it was possible to formulate a complete kinetic model that includes a rigorous mass and radiation balance.

(X) With a multi-parameter non-linear regression estimator, the few important missing kinetic constants were obtained.

(XI) Finally, computer simulations agreed very well with all the experimental data.

(XII) This outcome will be essential to describe, in the future, the more practical two-phase operating system.

Appendix I

Calculation of the spectral photonic fluence rate at the reactor windows

For the employed reactor with the recirculating loop it has been shown that for an isothermal, well mixed system (which means high recirculation rate), differential conversion per pass in the photoreactor and a ratio of $V_{R,irra}/V_{Tot} < 1$ the mass balance gives (Cassano and Alfano[33]):

$$\frac{dC_i(t)}{dt} = \frac{V_{R,irra}}{V_{Tot}} \left\langle R_i^{hom}(z,t) \right\rangle_{V_R} \tag{17}$$

where $V_{R,irra}$ is the irradiated volume (the photoreactor) and V_{Tot} the total volume of the system, R_i^{hom} is the homogeneous reaction rate, i is a reactant or a product and $\langle \ldots \rangle$ represents the volume averaging integral of the local rate over the photoreactor volume $V_{R,irra}$. For the batch reactor the initial condition is:

$$\text{at } t = 0,\ C_i = C_i^0 \tag{18}$$

For the employed reactor that has been considered one-dimensional and well-mixed, it can be shown that the averaging integral over $V_{R,irra}$ can be substituted by the average over L_R (the reactor length). For the actinometer (potassium ferrioxalate) the overall reaction is:

$$\left\langle R_\lambda^{act}(x,t) \right\rangle_{L_R} = \Phi_\lambda^{act} \left\langle e_{\lambda_{act}}^{a} \right\rangle_{L_R} \tag{19}$$

In eqn (19), $\left\langle e_{\lambda_{act}}^{a} \right\rangle_{L_R}$ is the average value of the local spectral volumetric rate of photon absorption (or the average of the local spectral absorbed flux density).

$$\frac{V_{Tot}}{V_{R,irra}} \left[\frac{dC_{Fe^{2+}}(t)}{dt} \right]_{T_K} = \Phi_\lambda^{act} \left\langle e_{\lambda_{act}}^{a} \right\rangle_{L_R} \tag{20}$$

For this reactor arrangement, with two windows and monochromatic radiation:

$$e_{\lambda_{act}}^{a}(z,t) = \alpha_{\lambda,act}(t) E_{\lambda,p,o,W} \left\{ \exp\left[-\alpha_{\lambda,Tot}(t) z\right] + \exp\left[-\alpha_{\lambda,Tot}(t)(L_R - z)\right] \right\} \tag{21}$$

In this equation $\alpha_{\lambda,Tot} = \alpha_{\lambda,Fe^{2+}} + \alpha_{\lambda,Fe^{3+}}$. In this case, at $t = 0$, $\alpha_\lambda^{Fe^{2+}}$ is 0. On the other hand, at $t = 0$ and $\lambda = 253.7$, $\alpha_\lambda^{Fe^{3+}}$ is very large. Then, combining eqn (20) with eqn (21) the spectral fluence rate at the reactor window is:

$$E_{\lambda,p,o,W} = \lim_{t \to 0} \left[\frac{(C_{Fe^{2+}} - C_{Fe^{2+}}^0)}{t - t^0} \right]_{T_K} \frac{V_{Tot}}{A_R \Phi_\lambda^{act}} \tag{22}$$

$C_{Fe^{3+}}$, $C_{Fe^{2+}}{}^0$ and t are measured and V_{tot}, A_R and $\Phi_\lambda{}^{act}$ are known. Thus eqn (22) gives the value of the spectral fluence rate at the reactor windows. Since the employed radiation is monochromatic, in the text the subscript λ has been omitted. Fig. 16 shows a typical actinometer result, and Table 5 summarises all results.

Table 5 Spectral fluence rate at the reactor windows

$E_{\lambda,0,W}$ (einstein cm^{-2} s^{-1})	
2 lamp Philips TUV 15 W	2.14×10^{-8}
2 lamp Heraeus 40 W	5.37×10^{-8}
2 lamp Heraeus 40 W with neutral density filters	1.16×10^{-8}
Percent transmittance of filter	21.60%

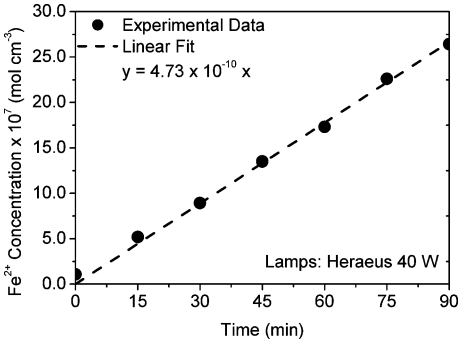

Fig. 16 Typical actinometer result.

Notation

V	Volume (cm^{-3})
$E_{\lambda,p,0}$	Spectral photon fluence rate (einstein cm^{-2} s^{-1})
$(E_{p,0,W})$	Photon fluence rate at the reactor windows (einstein cm^{-2} s^{-1}) (for monochromatic radiation)
$e_\lambda{}^a(x,t)$	Spectral photon radiation absorption power density or local volumetric rate of photon absorption (einstein cm^{-3} s^{-1})
$(\kappa C_{Oz}{}^0 L_R)$	Optical thickness (dimensionless)
C	Concentration (mol cm^{-3})
L	Length (cm)
R	Reaction rate (mol cm^{-3} s^{-1})
k	Kinetic constant. Units vary with the reaction order
$k_L a$	Volumetric mass transfer coefficient (s^{-1})
t	Time (s)
z	Spatial coordinate (cm)

Greek letters

κ	Molar Naperian absorption coefficient (cm^2 mol^{-1})
α	Linear Naperian absorption coefficient (cm^{-1})
λ	Wavelength (nm)
Φ_p	Primary quantum yield (mol einstein^{-1})

Subscripts

irra	Relative to irradiated volume
dark	Relative to dark volume
R	Relative to the reactor
Tot	Relative to total volume, or total species
i	Relative to the "i" reacting species
j	Relative to the "j" reaction step
p	Relative to a spatial point "p"
W	Relative to the reactor window
O_3	Relative to ozone
DCA	Relative to dichloroacetic acid
H_2O_2	Relative to hydrogen peroxide

Fe^{2+} Relative to ferrous ion
Fe^{3+} Relative to ferric ion

Superscripts

act Actinometer
0 Relative to the initial time ($t = 0$)

Special Symbols

$\langle \ldots \rangle$ Represents a volume average over the reaction space

Acknowledgements

The authors are grateful to Universidad Nacional del Litoral (UNL), Consejo Nacional de Investigaciones Científicas y Técnicas (CONICET), and Agencia Nacional de Promoción Científica y Tecnológica (ANPCyT) for the financial support.

References

1 C. Adams, T. Timmons and T. Seitz, Trihalomethane and haloacetic acid disinfection by-products in full-scale drinking water systems, *J. Environ. Eng.*, 2005, **131**, 526–534.
2 J. Lou, T. Chang and C. Huang, Effective removal of disinfection by-products and assimilable organic carbon: An advanced water treatment system, *J. Hazard. Mater.*, 2009, **172**, 1365–1371.
3 J. Kim, Y. Chung, D. Shin, M. Kim, Y. Lee, Y. Lim and D. Lee, Chlorination by-products in surface water treatment process, *Desalination*, 2002, **151**, 1–9.
4 K. Wang, J. Guo, M. Yang, H. Junji and R. Deng, Decomposition of two haloacetic acids in water using UV radiation, ozone and advanced oxidation processes, *J. Hazard. Mater.*, 2009, **162**, 1243–1248.
5 EPA Guidance Manual, *Alternative Disinfectants and Oxidants, Disinfectant Use in Water Treatment*, Washington, D.C., 1999, Chapter 2.
6 C. Zalazar, M. Labas, R. Brandi and A. Cassano, Dichloroacetic acid degradation employing hydrogen peroxide and UV radiation, *Chemosphere*, 2007, **66**, 808–815.
7 G. Peyton and W. Glaze, Destruction of pollutants in water with ozone in combination with ultraviolet radiation, *Environ. Sci. Technol.*, 1988, **22**, 761–767.
8 T. Garoma, M. Gurol, L. Thotakura and O. Osibodu, O., Degradation of tert-butyl formate and its intermediates by an ozone/UV process, *Chemosphere*, 2008, **73**, 1708–1715.
9 S. Song, Z. Liu, Z. He, Y. Li, J. Chen and C. Li, Degradation of the biocide 4-chloro-3,5-dimethylphenol in aqueous medium with ozone in combination with ultraviolet irradiation: Operating conditions influence and mechanism, *Chemosphere*, 1999, **77**, 1043–1051.
10 A. López-López, J. Pic and H. Debellefontaine, Ozonation of azo dye in a semi-batch reactor: A determination of the molecular and radical contributions, *Chemosphere*, 2007, **66**, 2120–2126.
11 J. Prado, J. Arantegui, E. Chamarro and S. Esplugas, Degradation of 2,4-D by ozone and light, *Ozone: Sci. Eng.*, 1994, **16**, 235–245.
12 P. Westerhoff, G. Aiken, G. Amy and J. Debroux, Relationships between the structure of natural organic matter and its reactivity towards molecular ozone and hydroxyl radicals, *Water Res.*, 1999, **33**, 2265–2276.
13 T. Lesko, A. Colussi and M. Hoffmann, Hydrogen Isotope Effects and Mechanism of Aqueous Ozone and Peroxone Decompositions, *J. Am. Chem. Soc.*, 2004, **126**, 4432–4436.
14 I. Fábián, Reactive intermediates in aqueous ozone decomposition: A mechanistic approach, *Pure Appl. Chem.*, 2006, **78**, 1559–1570.
15 T. Garoma and M. Gurol, Modeling Aqueous Ozone/UV Process Using Oxalic Acid as a Probe Chemical, *Environ. Sci. Technol.*, 2005, **39**, 7964–7969.
16 M. Lucas, J. Peres, B. Yan Lan and G. Li Puma, Ozonation kinetics of winery wastewater in a pilot-scale bubble column reactor, *Water Res.*, 2009, **43**, 1523–1532.
17 Y. Rao and W. Chu, A new approach to quantify the degradation kinetics of linuron with UV, Ozonation and UV/O_3 processes, *Chemosphere*, 2009, **74**, 1444–1449.
18 G. Gordon and B. Bubnis, Residual Ozone Measurement: Indigo Sensitivity Coefficient Adjustment, *Ozone: Sci. Eng.*, 2002, **24**, 17–28.
19 *Standard Methods for the Examination of Water and Wastewater*, ed. A. Eaton, L. Clesceri and A. Greenberg, Washington, 19th edition, 1995.
20 O. Allen, C. Hochnadel, J. Ghormley and T. Davis, Decomposition of water and aqueous solutions under mixed fast neutron and gamma radiation, *J. Phys. Chem.*, 1952, **56**, 575–586.
21 S. Murov, I. Carmichael, G. Hayon, *Handbook of Photochemistry 2nd Edition*, Marcel Dekker, New York, 1993.
22 P. Ausloos and E. Steacie, The Photolysis of Methy Ethyl Ketone, *Can. J. Chem.*, 1955, **33**, 1062–1068.
23 D. Singleton, G. Paraskevopoulos and R. Irwin Singleton, Laser Photolysis of Carboxylic Acids in the Gas Phase. Direct Determination of the OH Quantum Yield at 222 nm, *J. Phys. Chem.*, 1990, **94**, 695–699.
24 C. Zalazar, M. Lovato, M. Labas, R. Brandi and A. Cassano, Intrinsic Kinetics of the oxidative reaction of dichloroacetic acid employing hydrogen peroxide and ultraviolet radiation, *Chem. Eng. Sci.*, 2007, **62**, 5840–5853.
25 M. Lovato, C. Martin and A. Cassano, A reaction kinetic model for ozone decomposition in aqueous media valid for neutral and acidic pH, *Chem. Eng. J.*, 2009, **146**, 486–497.
26 A. Latifoglu and M. Gurol, The effect of humic acids on nitrobenzene oxidation by ozonation and O_3/UV processes, *Water Res.*, 2003, **37**, 1879–1889.
27 R. Buhler, J. Staehelin and J. Hoigné, Ozone Decomposition in Water studied by Pulse Radiolysis. 1. HO_2/O_2 - and HO_3/O_3 - as intermediates, *J. Phys. Chem.*, 1984, **88**, 2560–2564 and erratum.
28 F. Beltrán, *Ozone Reaction Kinetics for Water and Wastewater Systems*, Lewis Publishers Inc., New York, (2003).
29 F. Rivas, F. Beltrán, O. Gimeno and M. Carbajo, Fluorene Oxidation by Coupling of Ozone, Radiation and Semiconductors: A Mathematical Approach to the Kinetics, *Ind. Eng. Chem. Res.*, 2006, **45**, 166–174.
30 T. Garoma and M. Gurol, Degradation of tert-Butyl Alcohol in Dilute Aqueous Solution by an O_3/UV Process, *Environ. Sci. Technol.*, 2004, **38**, 5246–5252.
31 G. Rossetti, E. Albizzati and O. Alfano, Decomposition of Formic Acid in a Water Solution Employing the Photo-Fenton Reaction, *Ind. Eng. Chem. Res.*, 2002, **41**, 1436–1444.
32 M. Gurol and P. Singer, Kinetics of ozone decomposition: A dynamic approach, *Environ. Sci. Technol.*, 1982, **16**, 377–383.
33 A. Cassano and O. Alfano, Reaction engineering of suspended solid heterogeneous photocatalytic reactors, *Catal. Today*, 2000, **58**, 167–197.
34 H. Tomiyasu, H. Fukutomi and G. Gordon, Kinetics and mechanism of Ozone decomposition y basic aqueous solution, *Inorg. Chem.*, 1985, **24**, 2962–2966.
35 K. Sehested, J. Holcman and E. Hart, Rate constants and products of the reactions of e_{aq}^-, O_2^-, and H with Ozone in aqueous solutions, *J. Phys. Chem.*, 1983, **87**, 1951–1954.
36 Staehelin, R. Bühler and J. Hoigné, Ozone decomposition in water studied by pulse radiolysis. 2. OH and HO_4 as chain intermediates, *J. Phys. Chem.*, 1984, **88**, 5999–6004.
37 Christensen, K. Sehested and H. Corfitzen, Reactions of hydroxyl radicals with hydrogen peroxide at ambient and elevated temperatures, *J. Phys. Chem.*, 1982, **86**, 1588–1590.
38 Buxton, C. Greenstock, H. Phyllip and A. Ross, Critical review of Rate Constants for Reactions of Hydrated Electrons, Hydrogen Atoms and Hydroxyl Radicals (*OH/*O-) in Aqueous Solution, *J. Phys, Chem. Ref. Data*, 1988, **17**, 513–886.
39 B. Bielski and A. Allen, Mechanisms of disproportionation of superoxide radicals, *J. Phys. Chem.*, 1977, **81**, 1048–1050.
40 M. Gurol and A. Akata, Kinetics of Ozone Photolysis in Aqueous Solution, *AIChE J.*, 1996, **42**, 3283–3292.
41 Baxendale and J. Wilson, The photolysis of hydrogen peroxide at high light intensities, *Trans. Faraday Soc.*, 1957, **53**, 344–356.

